

Dosimetric leaf gap and leaf trailing effect in a double-stacked multi-leaf collimator

1
2

3 Victor Hernandez^{1,2}

4 Department of Medical Physics, Hospital Sant Joan de Reus, IISPV, 43204 Tarragona,
5 Spain

6 Jordi Saez¹

7 Department of Radiation Oncology, Hospital Clínic de Barcelona, 08036 Barcelona, Spain

8 Agnes Angerud

9 RaySearch Laboratories AB, Stockholm, Sweden

10 Romain Cayez

11 Department of Medical Physics, Oscar Lambret Center, 59000 Lille, France

12 Catherine Khamphan

13 Medical Physics Department, Institut Sainte-Catherine, 84000 Avignon, France

14 Daniel Nguyen

15 Centre de Radiothérapie de Mâcon, 71000 Mâcon, France

16 Laure Vieillevigne

17 Department of Medical Physics, Institut Claudius Regaud—Institut Universitaire du
18 Cancer de Toulouse, 31059 Toulouse, France

19 Centre de Recherche et de Cancérologie de Toulouse, UMR1037 INSERM, Université
20 Toulouse 3, ERL5294 CNRS, Oncopole, 31037 Toulouse, France

21 Vladimir Feygelman

22 Department of Radiation Oncology, Moffitt Cancer Center, Tampa, 12902 Florida, USA

23 ¹ The first two authors contributed equally to this work

24 ² Author to whom correspondence should be addressed.

25 email: vhernandezmasgrau@gmail.com

26 Hospital Sant Joan de Reus

27 Av. del Dr. Josep Laporte, 2

28 43204 Reus, Tarragona, Spain

29 Short running title: DLG and trailing effect in a stacked MLC

This article has been accepted for publication and undergone full peer review but has not been through the copyediting, typesetting, pagination and proofreading process, which may lead to differences between this version and the [Version of Record](#). Please cite this article as [doi: 10.1002/MP.14914](https://doi.org/10.1002/MP.14914)

This article is protected by copyright. All rights reserved

Abstract

Purpose: To investigate (i) the dosimetric leaf gap (DLG) and the effect of the ‘trailing distance’ between leaves from different multi-leaf collimator (MLC) layers in HalcyonTM systems and (ii) the ability of the currently available treatment planning systems (TPS) to approximate this effect.

Methods: DICOM plans with transmission beams and sweeping gap tests were created in Python for measuring the DLG for each MLC layer independently and for both layers combined. In clinical Halcyon plans both MLC layers are interchangeably used and leaves from different layers are offset, thus forming a trailing pattern. To characterize the impact of such configuration, new tests called ‘trailing sweeping gaps’ were designed and created where the leaves from one layer follow the leaves from the other layer at a fixed ‘trailing distance’ t between the tips. Measurements were carried out on five Halcyons SX2 from different institutions and calculations from both the Eclipse and RayStation TPSs were compared with measurements.

Results: The dose accumulated during a sweeping gap delivery progressively increased with the trailing distance t . We call this ‘the trailing effect’. It is most pronounced for t between 0 and 5 mm, although some changes were obtained up to 20 mm. The dose variation was independent of the gap size. The measured DLG values also increased with t up to 20 mm, again with the steepest variation between 0 and 5 mm. Measured DLG values were negative at $t=0$ (the leaves from both layers at the same position) but changed sign for $t \geq 1$ mm, in line with the positive DLG sign usually observed with single-layer rounded-end MLCs. The Eclipse TPS does not explicitly model the leaf tip and, as a consequence, could not predict the dose reduction due to the trailing effect. This resulted in dose discrepancies up to +10% and -8% for the 5 mm sweeping gap and up to $\pm 5\%$ for the 10 mm one depending on the distance t . RayStation implements a simple model of the leaf tip that was able to approximate the trailing effect and improved the agreement with measured doses. In particular, with a prototype version of RayStation that assigned a higher transmission at the leaf tip the agreement with measured doses was within $\pm 3\%$ even for the 5 mm gap. The five Halcyon systems behaved very similarly but differences in the DLG around 0.2 mm were found across different treatment units and between MLC layers from the same system. The DLG for the proximal layer was consistently higher than for the distal layer, with differences ranging between 0.10 mm and 0.24 mm.

Conclusions: The trailing distance between the leaves from different layers substantially affected the doses delivered by sweeping gaps and the measured DLG values. Stacked MLCs introduce a new level of complexity in TPSs, which ideally need to implement an explicit model of the leaf tip in order to reproduce the trailing effect. Dynamic tests called ‘trailing sweeping gaps’ were designed that are useful for characterizing and commissioning dual-layer MLC systems.

The table of contents is for drafting and refereeing purposes only. Note that all links to references, tables and figures can be clicked on and returned to calling point using cmd[on a Mac using Preview or some equivalent on PCs (see View - go to on whatever reader).

Contents

I. Introduction	1
II. Materials and Methods	2
II.A. Halcyon system and MLC characteristics	2
II.B. Tests and experiments	3
II.C. Equipment and measurements	4
II.D. Description of the TPS MLC models	5
III. Results	6
III.A. Dosimetric leaf gap and MLC transmission	6
III.B. Effect of the leaf trailing distance (trailing effect)	8
III.C. Modeling the trailing effect in the TPSs	9
IV. Discussion	11
V. Conclusions	15
References	16

1. Introduction

A fast-rotating, enclosed, ring-mounted gantry system designed for intensity modulated radiotherapy/volumetric modulated arc therapy (IMRT/VMAT) delivery, the Halcyon (Varian Medical Systems, Palo Alto, CA), has been recently released^{1,2}. The system incorporates some unique features different from traditional C-arm linacs, including a dual-layered stacked and staggered multi-leaf collimator (MLC). Its innovative design offers attractive features but also raises new challenges and requires some adaptation of the commissioning procedures^{3,4}.

The Halcyon is delivered with the Eclipse treatment planning system (TPS) from the same manufacturer (Varian Medical Systems), which includes a fully pre-configured photon beam model based on the reference beam data. Extensive validation tests have been performed and installed systems have been found to accurately match the reference beam data preconfigured in Eclipse, including percentage depth doses, profiles, and output factors^{3,5}. It has also been reported that the system complies with commissioning criteria from international guidelines^{6,7,8,9,10,11} and a good agreement between measurements and calculations for clinical plans was found in patient-specific quality assurance (QA) tests, end-to-end verifications and external audits^{2,3,12}.

RayStation (RaySearch Laboratories, Stockholm, Sweden), a TPS independent of treatment units' manufacturers, is also commercially available for the Halcyon. Saini et. al.¹² recently showed that RayStation provides excellent dose calculation accuracy for the Halcyon, offering the possibility to integrate equipment from different manufacturers in a clinical workflow. RayStation does not include any pre-configured beam model, thus requiring a more comprehensive data collection and commissioning effort.

In clinical plans for the Halcyon, leaves from the stacked layers closely follow one another to further reduce the interleaf leakage compared to the standard single-layer design. We will call the distance between the tips of the leaves from stacked layers the 'trailing distance'. The basic characteristics of the Halcyon's dual-layer MLC, such as leaf positioning reproducibility, transmission, and the dosimetric leaf gap (DLG¹³), which accounts for the transmission through the rounded leaf ends, have been reported^{14,15}. However, all the studies to date investigated simplified geometries with either a single MLC layer or both layers with the same nominal leaf positions defining the aperture. This simplification is not generally applicable

117 to the clinical treatment plans. To achieve maximum fluence conformality (i.e. effective leaf
118 width of 5 mm), the leaves from different layers must be offset somewhat when defining a
119 curved aperture, thus forming a trailing pattern. Lim et al¹⁵ postulated that leaf trailing
120 could affect dose calculation accuracy, particularly for the highly modulated plans. However,
121 how the trailing distance affects the effective transmission through the leaf tips has not been
122 investigated in detail so far. Moreover, some authors have reported DLG values of opposite
123 signs for certain aperture configurations^{12,14}, raising the conceptual question of the meaning
124 of the DLG for the double-stacked MLC. The interplay between the MLC layers certainly
125 presents new challenges in MLC modeling.

126 The primary goals of this study are to quantitate the dosimetric leaf gap in the presence
127 of leaves from different MLC layers trailing each other and its effect on the dose calculations
128 in the two TPSs currently supporting Halcyon. Secondary goals are to determine the consis-
129 tency of the dosimetric leaf gap and the trailing effect across a number of Halcyon systems
130 and to evaluate the feasibility of using a common preconfigured MLC model in the TPS.

131 II. Materials and Methods

132 II.A. Halcyon system and MLC characteristics

133 The HalcyonTM system consists of a single-energy 6 MV flattening filter free linear accelera-
134 tor that is isocentrically mounted on a covered fast-rotating ring gantry with a source-to-
135 isocenter distance of 100 cm. The system is equipped with a stacked-and-staggered dual-layer
136 MLC composed of 29 proximal leaf pairs ('upper' layer) and 28 distal leaf pairs ('lower' layer)
137 that can produce a maximum field size of $28 \times 28 \text{ cm}^2$ at the isocenter plane. Leaves have a
138 projected width of 1 cm, a maximum leaf speed of 5 cm/s and travel across the full 28 cm
139 range (all values at the isocenter plane). The proximal layer is offset by 5 mm along the
140 leaf width from the distal one. The first release of the Halcyon, version SX1, performed
141 the field shaping with the distal leaves only, whereas the proximal leaves merely served as a
142 backup collimator in order to reduce transmission. Halcyon SX2, on the contrary, performs
143 the field shaping with both leaf layers independently, allowing for a finer shaping of the field
144 apertures and reducing the effective leaf widths at the isocenter plane to 5 mm^{1,15}.

145 Both MLC layers are focused only in the direction perpendicular to the leaf motion and

146 the leaf ends are rounded. The curvature radius is 23.4 cm, which is larger than the radius for
147 the standard Varian MLCs (8 cm and 16 cm for the Millennium and High-Definition MLCs,
148 respectively). The leaves are also taller than in the other Varian MLCs (7.7 cm compared
149 with 6.50-6.75 cm), contributing to a lower MLC transmission through a single leaf.

150 II.B. Tests and experiments

151 Sweeping gaps and transmission measurements were used to determine the DLG. The DLG
152 is commonly used for the dosimetric characterization of the leaf tip¹³ and accounts for the
153 leaf position calibration and additional transmission through the rounded leaf ends^{13,16}. Two
154 types of DLG tests were devised for each MLC layer. The first one involved one MLC layer at
155 a time and essentially duplicated the classical setup described for the single-layer MLCs. The
156 second set of tests was designed to investigate the impact of the trailing distance between
157 leaves from different MLC layers.

158 DICOM RT Plan files for the DLG determination were created in Python 3.7 with the
159 MLC defining a rectangular aperture of a certain width or ‘gap size’ and a 10 cm length.
160 Leaves moved at the same constant speed between all control points and for all gap sizes.
161 The gap center moved from -6 cm to $+6$ cm with 13 control points, such that the shift in
162 leaf positions between consecutive control points was 1 cm. The other MLC layer’s leaves
163 were kept fixed at ± 5 cm in order to crop the beam aperture to the central 10×10 cm² square
164 region. By using this arrangement, the leaves fixed at ± 5 cm mimic the jaws commonly used
165 in DLG measurements with Varian linacs, thus keeping the same scatter conditions. This
166 configuration is illustrated in Fig. 1a. Two sets of gap sizes were defined: an extended set
167 with gap sizes from 2 mm to 20 mm in 2 mm steps and a reduced set with gap sizes of 2, 5,
168 10, 15 and 20 mm. For comparison purposes, the DLG was also measured with the DICOM
169 files provided by the manufacturer.

170 To investigate the impact of the trailing distance between leaves from different MLC
171 layers, a variation of the sweeping gap test that we named ‘trailing sweeping gaps’ (tSGs)
172 was designed where the leaves from each layer were separated by a fixed distance (a sketch
173 is provided online as Supporting Information). While the leaves from one layer define the
174 sweeping gap and move according to the classical sweeping sequence (these are the leading
175 leaves), the leaves from the other layer follow them at a fixed trailing distance tip to tip

(these are the trailing leaves). To characterize this effect, experiments were performed for trailing distances of 0, 0.5, 1, 2, 3, 4, 5, 10 and 20 mm, fully covering the region spanned by the leaf tip widths, and were carried out twice, with reversed roles of trailing and leading layers. Since the transmission through both MLC layers simultaneously is practically negligible¹⁵, only a fixed width of twice the trailing distance (one at each side of the sweeping gap aperture) effectively contributes to the transmission in these tests. Therefore, this transmission component is independent of the gap size and was directly measured away from the leaf tip. To crop the beam aperture to the central $10 \times 10 \text{ cm}^2$ square region, the trailing leaves were kept at a maximum off-axis distance of 5 cm. Additionally, the sweeping gap size beyond this position was reduced to 1 mm in order to minimize transmission and scatter while fulfilling the minimum dynamic leaf gap of 0.5 mm. In these tests, a higher number of control points was used (between 25 and 27 depending on the gap size) to produce this cropped configuration while keeping the same constant leaf speed in the central $10 \times 10 \text{ cm}^2$ region. The trailing sweeping gap test is sketched in Fig. 1b.

The MLC transmission was measured for each MLC layer and leaf bank (right A or left B) individually for the $10 \times 10 \text{ cm}^2$ and several other field sizes. For each field size, measurements were carried out with the open beam and the beam closed by a different MLC bank. The transmission for each layer and field size was computed as the ratio of the average reading through the closed banks over the reading for the same size open beam.

The number of delivered monitor units (MU) ranged between 200 and 300, which produced leaf speeds below 1 cm/s. The DICOM files for the tests will be provided by the authors upon request.

II.C. Equipment and measurements

All the experiments were conducted on five Halcyon SX2 systems from different institutions. Two institutions used the Eclipse, two used RayStation and one institution used both Eclipse and RayStation. Details of the participating institutions, equipment and systems used are given in Table 1.

Measurements were performed either in water or in a water-equivalent plastic phantom and all centers used a Farmer chamber PTW 30013. Other detectors can be used for measur-

205 ing the DLG but the Farmer chamber is recommended because it provides a good assessment
206 of the average dose due to its relatively large size^{13,17}. Measurements were carried out at
207 a source-to-surface distance of 90 cm, with the chamber placed at the isocenter at a 10 cm
208 depth.

209 The DLG was determined from the chamber readings with the sweeping gaps. The
210 MLC transmission component was subtracted from each reading. Next, a linear fit of the
211 corrected readings as a function of the nominal gap size was performed. Finally, the DLG
212 was defined as the negative of the gap axis intercept of this linear fit, such that a negative
213 intercept sign corresponds to a positive DLG and vice versa^{13,18}.

214 All the Halcyon systems and TPSs used in this study were carefully commissioned
215 according to international guidelines^{6,7,8,10,11}. Calculations were carried out with the dose
216 calculation algorithms clinically used at each institution (see Table 1). Two calculation
217 grid resolutions were evaluated: 2.5 mm, which is commonly used in clinical practice,¹⁹ and
218 1 mm, which is the finest resolution available in both TPSs. Calculated doses were obtained
219 as the average doses over a delineated cylindrical structure mimicking the active volume of
220 the Farmer chamber. Calculated doses (D_{calc}) were compared with measured doses (D_{meas})
221 and differences were computed as $(D_{\text{calc}} - D_{\text{meas}})/D_{\text{meas}}$ and expressed as percentage values.

222 II.D. Description of the TPS MLC models

223 The Eclipse TPS uses three parameters to model the MLC: the DLG, the MLC transmis-
224 sion, and the tongue-and-groove width. Calculations in Eclipse are carried out considering
225 all leaves with flat tips retracted by $DLG/2$ with respect to the nominal leaf positions. By
226 applying this shift, the additional transmission through the rounded leaf end can be ap-
227 proximately compensated for and the integral fluence in the sweeping gap beams can be
228 reproduced. The MLC transmission is defined for each MLC layer as the average leaf trans-
229 mission and the tongue-and-groove width is subtracted from the fluence map at the exposed
230 sides of the leaves^{20,21}. The MLC model in Eclipse for the Halcyon uses a $DLG = 0.1$ mm,
231 a transmission for a single MLC layer of 0.47% and a null transmission below both MLC
232 layers. The tongue-and-groove widths for the proximal and distal layers are 0.56 mm and
233 0.40 mm, respectively. All these parameters are fixed and unmodifiable by the user²².

234 The MLC model in RayStation has several user-definable parameters: leaf tip width,
235 x-offset, MLC transmission, tongue-and-groove width, gain and curvature. The MLC trans-
236 mission indicates the average transmission for a single MLC layer and a null transmission
237 below both layers is considered. The leaf is represented in the model as a heightless rectangle
238 with the defined transmission. The leaf tip width parameter defines a region near the tip
239 where a constant transmission equal to \sqrt{T} is assigned. A similarly reduced transmission
240 is also assigned to the tongue-and-groove regions extending from the exposed leaf sides.
241 Additionally, an effective leaf position is considered in the calculations where all leaves are
242 shifted by a certain amount which at the central axis is equal to the ‘x-offset’ parameter and
243 at the off-axis positions also depends on the ‘gain’ and ‘curvature’ parameters. A detailed
244 description of these parameters can be found in the RayStation 10A Reference Manual²³.

245 The most recent version of RayStation (RayStation 10A) was included in this study,
246 which implements separate configurations parameters for each MLC layer. Additionally, a
247 prototype version was also evaluated where the transmission assigned to the leaf tip region
248 was increased to a fixed value of 0.20 (corresponding to a 20% transmission). This prototype
249 version will hereafter be referred to as RayStation 11P.

250 III. Results

251 III.A. Dosimetric leaf gap and MLC transmission

252 The results for the DLG and MLC transmission values obtained at each institution are given
253 in Table 2. The average DLG value was 0.44 mm for the proximal layer (range 0.36-0.48 mm)
254 and 0.28 mm for the distal layer (range 0.12-0.38 mm). At all institutions the measured dis-
255 tal DLG was smaller than the measured proximal DLG, differing by 0.16 ± 0.05 mm (aver-
256 age ± 1 SD). In all cases the Pearson’s correlation coefficient r of the linear regression gave
257 $1-r^2$ values below 10^{-6} . The MLC transmission for a single layer was $0.33 \pm 0.01\%$ at all
258 institutions.

259 For the sweeping gap beams with both MLC layers defining the aperture (i.e. leaves
260 from both layers at the same position) the DLG ranged from -0.62 to -0.42 mm and was
261 -0.49 mm on average. This value was 0.93 mm smaller than the average DLG of the proximal
262 layer and 0.77 mm smaller than the average value of the distal layer. The MLC transmission

263 under both MLC layers was lower than 0.01% at all institutions (average of 0.005%), which
264 can be considered negligible for practical purposes. The corrected readings for a representa-
265 tive case (Institution A), including the linear fits and the DLG derivation for each layer and
266 both layers, are shown in Figure 2. The DLG values shown in Table 2 were obtained with
267 gap sizes varying by 2 mm. At all institutions the DLG values obtained with the reduced set
268 of gap sizes agreed within 0.01 mm with those measured with the extended set of gap sizes.
269 Note that a negative DLG value corresponds to a positive gap axis intercept of the linear fit
270 line (lower curve in Fig. 2).

271 For comparison purposes, the DLG and transmission were also determined with the
272 DICOM files provided by Varian, which only include the DLG set for the distal layer. The
273 DLG values obtained with these files differed from those obtained with our custom-made
274 ones. The average MLC transmission between all centers was $0.47 \pm 0.01\%$, which was
275 higher than the 0.34% value with the custom plan files. The DLG for the distal layer was
276 -0.34 ± 0.10 mm, which was smaller than the 0.28 mm previously determined.

277 The disparity in the MLC transmission values obtained with our files and the ones
278 provided by Varian was caused by the different field sizes used. The files provided by Varian
279 use a field size around 27×27 cm², which is close to the maximum field size for the Halcyon.
280 However, the values given in Table 2 were obtained with a 10×10 cm² field size (as defined
281 by the other MLC layer) and it is well known that the MLC transmission depends on
282 the field size²⁴. To further investigate this dependence, MLC transmission was measured
283 for various field sizes (5×5 , 15×15 , 20×20 and 25×25 cm²). As shown in Figure 3, MLC
284 transmission varied from approximately 0.31% to 0.47% as the field size increased from
285 5×5 cm² to 25×25 cm². Note that when the exact field size in the direction perpendicular
286 to the leaf motion could not be achieved due to the 1 cm leaf widths, slightly larger field
287 sizes were used in that direction and MLC transmission was referenced to the corresponding
288 equivalent square field.

289 A detailed analysis of the DICOM RT Plan files provided by Varian for the determination
290 of the DLG revealed that the distance travelled by the leaves depended on the gap size. The
291 leaves travelled 14.8 cm for the smallest gap size of 2 mm and this distance was progressively
292 reduced with the gap size, going down to 13 cm for the 20 mm gap. With a constant number
293 of MUs, such differences affect the leaf speed and thus the linearity of the corrected readings

294 as a function of the gap size, leading to the incorrect DLG values. Further details on the
295 loss of linearity and on the structure of the corresponding residuals from the linear fit are
296 provided online as Supporting Information.

297 III.B. Effect of the leaf trailing distance (trailing effect)

298 The DLG was also determined with the trailing sweeping gap tests, in which a certain trailing
299 tip to tip distance is kept between the leading layer defining the gap size and the trailing
300 layer. The results are reported specifying the leading layer used in each case: ‘proximal layer’
301 indicates that the proximal leaves were leading, with distal leaves trailing, and vice versa.
302 As shown in Figure 4, the DLG exhibited a strong dependence on the trailing distance. For
303 a zero trailing distance, the projections of leaves from each layer coincide and both layers
304 define the sweeping gap simultaneously. In this case, a negative DLG was obtained (Table 2).
305 The DLG increased with the trailing distance up to ~ 10 mm, after which it reached a plateau
306 close to the single layer DLG value given in Table 2.

307 All five Halcyon systems exhibited the same behavior and differences between the curves
308 were only due to the variations in the DLG values at different institutions (Table 2). To
309 illustrate this similarity, all the curves were vertically shifted to match a common average
310 DLG for each layer at the 20 mm trailing distance. This resulted in overlapping curves (see
311 Figure 4c).

312 The variations in the DLG for the tSG tests were caused by differences in the doses
313 measured for different trailing distances. The measured sweeping gap doses as a function
314 of the trailing distance at a representative institution (center E) are illustrated in Figure 5.
315 As the trailing distance decreased, the sweeping gap doses were progressively reduced. For
316 trailing distances between 20 mm and 5 mm this reduction was small and nearly linear, while
317 for trailing distances below 5 mm the dose reduction was larger and progressively steeper.

318 The dose variations shown in Figure 5 were independent of the gap size; therefore,
319 the linear fit line used to determine the DLG (corrected readings as a function of the gap
320 size in Fig. 2) was shifted downwards as the trailing distance was reduced, resulting in a
321 lower (more negative) DLG value. Since the dose variations were the same for all gap sizes,
322 the corresponding relative variations ended up much higher for the small gaps: the relative

323 variation between the trailing distances of 0 and 5 mm was approximately 5% for the 20 mm
324 gap, 10% for the 10 mm gap, and as high as 20% for the 5 mm gap. The dose versus trailing
325 distance curves at all centers were very similar, with only a scaling difference due to the
326 different calibration setups (associated with nominal dose rates) and each machine-specific
327 DLG.

328 To investigate the reason behind this effect, the variation of the transmission through the
329 leaf ends for different trailing distances was investigated by ray tracing computations. The
330 results for direct transmission considering photons with a vertical (non divergent) incidence
331 and a simple exponential attenuation through the leaves are given in Figure 6, where a linear
332 attenuation coefficient $\mu = 0.74 \text{ cm}^{-1}$ was chosen to obtain a transmission of 0.33% for a leaf
333 height of 7.7 cm. As the projections of the leaves from each layer get closer, the additional
334 fluence through the rounded leaf ends is reduced due to the combined attenuation from
335 both leaves. Thus, when the leaf projections coincide (trailing distance = 0), the transmitted
336 photons must pass through the leaf tips from both layers, which increases attenuation and
337 reduces the DLG.

338 Figure 6 illustrates the transmission computed with ray tracing for different trailing
339 distances, as well as the corresponding integral transmission and equivalent offset. The inte-
340 gral transmission was obtained from accumulating the transmission profile and subtracting
341 the transmission corresponding to that of flat and double-focused leaves, hence the offset
342 indicates the leaf tip transmission component to the DLG¹⁶. The intrinsic DLG can be
343 computed as twice this offset¹⁶ and strongly depends on the trailing distance (see Fig. 6c),
344 which approximately explains the variation in the measured DLG. For further details on the
345 relationship between the DLG, the integral transmission and the offset, the readers are re-
346 ferred to Arnfield et al¹⁶. This offset has also been called intrinsic offset and its relationship
347 with the ‘x-offset parameter’ in RayStation was recently provided by Saez et al¹⁷.

348 III.C. Modeling the trailing effect in the TPSs

349 The sweeping gap and trailing sweeping gap plans were imported and calculated in Eclipse
350 and RayStation. The calculated doses and the derived DLG values were compared to the
351 experiments.

352 The calculated doses for the sweeping gaps in Eclipse were independent of the MLC
353 layer and varied slightly with the trailing distance. As shown in Figure 7, the calculated
354 dose varied linearly with the trailing distance and Eclipse underestimated the dose for trailing
355 distances $\gtrsim 1$ mm and overestimated it for trailing distances $\lesssim 1$ mm. Differences depended
356 on the gap size and were as high as +10% and -8% for the 5 mm gap and $\pm 5\%$ for the
357 10 mm gap.

358 The results in RayStation depended on the version used. In version 10A the calculated
359 doses varied smoothly for trailing distances t larger than the ‘leaf tip width’ parameter
360 configured in the system and showed a more pronounced variation for trailing distances
361 below this value (see dashed lines in Fig. 7). The TPS underestimated the dose for $t \gtrsim 1$ mm,
362 with differences around -3%, and overestimated the dose for $t \lesssim 1$ mm with discrepancies
363 up to +9%. This represented a clear improvement with respect to Eclipse for $t \gtrsim 1$ mm
364 (discrepancies were approximately halved) but only a minor improvement for $t \lesssim 1$ mm.

365 In RayStation 11P the dose increase between trailing distance = 0 and trailing distance
366 equal to the ‘leaf tip width’ was steeper (dotted lines in Fig. 7) due to the higher transmission
367 (20%) assigned to this region compared to the previous value of \sqrt{T} (5.7% for $T = 0.33\%$).
368 This resulted in a better agreement across the entire range of trailing distances. The only
369 substantial differences with the measured doses were obtained between $t = 0.5$ mm and 3 mm
370 but all differences were within $\pm 1\%$, $\pm 2\%$, and $\pm 3\%$ for the gap sizes of 20 mm, 10 mm and
371 5 mm, respectively.

372 The calculated doses were independent of the grid size in both TPSs. Figure 7 shows
373 the measured and calculated doses for the 10 mm sweeping gap. Sweeping gaps of other sizes
374 produced similar dose variations, but the relative dose differences depended on the gap size:
375 the smaller the gap size, the larger the relative dose difference. More information on other
376 gap sizes and their corresponding dose differences is provided as Supporting Information
377 (Figures S3, S4 and S5).

378 To better characterize the modeling of the trailing effect a ‘calculated DLG’ was de-
379 rived from the calculated doses and compared with the measured DLG. The calculated DLG
380 from Eclipse was 0.13 ± 0.01 mm for all the tests regardless of the MLC layer, of the trailing
381 distance and of the version of Eclipse (Fig. 8). This 0.13 mm value was only slightly larger
382 than the fixed 0.10 mm parameter preconfigured in the TPS. The DLG from RayStation 10A

383 decreased somewhat for small trailing distances, but not sufficiently to match the experi-
384 ment. RayStation 11P exhibited a steeper variation in the DLG for small trailing distances,
385 which improved the agreement between the calculated and measured DLG for large trailing
386 distances (single layer DLG) as well as for a trailing distance $t=0$ (DLG for both layers
387 combined).

388 IV. Discussion

389 The Halcyon™ has a double-layer MLC and in v2.0 clinical plans the leaf positions from
390 both layers are kept as close as possible to achieve the effective 5 mm resolution, as well
391 as to reduce the effective MLC transmission. The leaves from one MLC layer follow the
392 leaves from the other layer at a close ‘trailing’ distance with proximal and distal layers
393 interchangeably taking leading and trailing roles. The trailing distance t affects the doses
394 delivered by dynamic fields; hence the stacked MLC introduces new characterization and
395 modeling challenges.

396 As the trailing distance t was increased, the doses delivered by the sweeping gaps in-
397 creased. For $t > 5$ mm the increase was nearly linear with t , corresponding only to the added
398 transmission of one layer compared to two, and did not affect the measured DLG values.
399 However, as the trailing distance was reduced below 5 mm, there was a steeper decrease
400 in the measured doses and the corresponding DLG also decreased, which suggested some
401 modification of the effective transmission through the overlapping leaf tips.

402 We used a simple ray tracing code to show that such a trailing effect could be due to the
403 interplay between the attenuation at the leaf tips of both MLC layers and to the transmission
404 through their rounded leaf ends. When the trailing distance is zero, the leaves from both
405 layers define the gap size and the transmission through the leaf tips is reduced due to the
406 combined attenuation of two MLC layers. Without accounting for other phenomena such as
407 MLC scatter, source size or changes in the energy spectrum, simple ray tracing was sufficient
408 to qualitatively show the impact of the leaf trailing distance on the integral transmission and
409 on the DLG (see Fig. 6).

410 For the specific TPSs, Eclipse failed to model the steeper dose reduction for small
411 trailing distances ($t < 5$ mm). The reason for this is that Eclipse accounts for the additional

412 transmission through the rounded leaf end by retracting the leaf positions a certain distance
413 (DLG/2), but it does not implement any explicit model of the leaf tip, effectively considering
414 it flat. To better replicate the interplay between the leaf tips from different MLC layers, a
415 better MLC model for the Halcyon system would likely be necessary.

416 The main advantage of RayStation is that it includes a more detailed, although still
417 rudimentary, model of the leaf tip. It uses a two-step function where a constant intermediate
418 transmission is assigned to a certain length at the end of the leaf equal to the ‘leaf tip width’
419 parameter configured in the system. For trailing distances below the leaf tip width this
420 model produced a steeper dose reduction for the sweeping gap doses, as well as a linear
421 reduction in the corresponding DLG (see Figures 7 and 8). The best results were obtained
422 with RayStation 11P, because the higher transmission assigned to the leaf tip produced a
423 steeper dose variation for small trailing distances. RayStation 11P yielded an agreement
424 within $\pm 3\%$ even for the 5 mm sweeping gaps. To further improve this agreement a more
425 sophisticated leaf tip model would likely be required, which could go from the implementation
426 of a three-step function (with two intermediate transmission levels at the leaf tip instead of
427 only one) to a continuous variable transmission through the curved portion of the leaf.

428 The MLC transmission values obtained at all centers were consistent. For both MLC
429 layers combined the transmission was negligible ($\sim 0.005\%$) and for a single layer the trans-
430 mission varied between approximately 0.30% and 0.50% depending on the field size. For
431 the field sizes below $20 \times 20 \text{ cm}^2$, the MLC transmission for the proximal layer was smaller
432 than for the distal one, which can be plausibly explained by the former’s closer position to
433 the source (fewer scattered photons reaching the detector). However, Fig. 3 shows a slightly
434 greater transmission for the proximal layer for the $25 \times 25 \text{ cm}^2$ field size. The exact reason
435 for this reversal is unknown, but the differences were minimal and should have no practical
436 implications. Since in clinical plans the area shielded by only a single MLC layer is limited
437 to a small region around the beam aperture, it is reasonable to consider the average MLC
438 transmission in clinical plans to be close to 0.30%.

439 The DLGs measured in the present study were quite homogeneous across five institu-
440 tions. The DLG for the proximal layer was consistently higher on average than for the distal
441 layer by $0.16 \pm 0.05 \text{ mm}$, which should ideally be taken into account by the TPS. Some dif-
442 ference was expected because for the same physical leaf height and tip radius, the different

443 distance from each MLC layer to the isocenter plane impacts the trailing effect and the DLG.
444 The geometrical projection of the leaf tip width at the isocenter is larger for the proximal
445 layer. As a consequence, the plateau is reached at a larger trailing distance (see Figures 4-5)
446 and the DLG value of the proximal layer is larger compared to the distal one. The measured
447 DLGs for different treatment units ranged between 0.36 mm and 0.48 mm for the proximal
448 layer and between 0.12 mm and 0.38 mm for the distal layer. These results support the
449 assumption that a common preconfigured MLC model for the Halcyon system is feasible.
450 However, differences in the measured DLG around 0.2 mm were found, which are equivalent
451 to systematic differences of 0.1 mm in leaf positions. Such differences are experimentally
452 detectable in Halcyon plans and can produce average ion chamber point dose difference-
453 saround 0.8% in clinical cases¹². To minimize these differences, a slight modification of the
454 MLC modeling parameters should be allowed.

455 A wider range of DLG values for the Halcyon has been reported in the literature for
456 the distal layer, with values ranging between -0.23 and $+0.27$ mm^{2,3,12,15}. Kim et al.¹⁴
457 measured the DLG for single layers and both layers combined and reported a larger DLG for
458 both layers (0.96 mm) than for each single layer (-0.20 mm), which is the opposite of what
459 we found. We believe that these discrepancies are mainly due to methodological and perhaps
460 reporting differences, rather than to actual differences between the MLCs. It is important to
461 determine the DLG with sweeping gaps of all sizes traveling at the same speed; otherwise,
462 the linearity of the corrected readings as a function of the gap size is reduced and systematic
463 errors are introduced (see Fig. S1 in the Supporting Information). We also want to note that
464 with DLG values so close to zero it is necessary to carefully determine the sign of the DLG.

465 Negative DLG values are counterintuitive. The DLG accounts for the additional trans-
466 mission through the rounded leaf end and is expected to be positive for the leaf positions
467 calibrated by visible or infrared light. Negative values could in principle be due to differ-
468 ences between the leaf position origins of each MLC layer, but in reality such differences were
469 very small (<0.2 mm as estimated by additional measurements) and could not explain by
470 themselves the negative DLG values around -0.5 mm. We believe that another contributing
471 factor could be the photon source occlusion: when both MLC layers define the sweeping gap
472 (trailing distance close to zero), the combined source occlusion by each layer reduces the
473 sweeping gap doses and could contribute to a negative DLG.

474 Despite the large discrepancies found between calculated and measured doses for small
475 trailing distances, a good agreement in clinical plans has been reported for both Eclipse and
476 RayStation in patient-specific QA verifications, end-to-end tests and certification audits^{2,3,12}.
477 The reason for this is probably that the MLC models were configured with parameters that
478 partially compensate for the limitations in each TPS. Several authors have shown that the
479 DLG parameter that maximizes the clinical dose calculation accuracy may not necessarily
480 be the same as the measured DLG²⁵, which can be used to compensate for limitations in the
481 MLC model²⁶. Of note, the DLG value of 0.1 mm preconfigured in Eclipse is an intermediate
482 value between the DLG per layer and for both layers (see straight line in Fig. 8). This value is
483 probably a good compromise for Eclipse that provides acceptable accuracy in typical clinical
484 plans. Of course the influence of the trailing interplay is reduced, as any other leaf penumbra
485 effect, in the clinical plans containing a relatively large proportion of wide apertures.

486 Such compromises are, however, not optimal. The ‘optimal’ configuration parameters
487 may depend on the characteristics of each individual clinical plan and, as a consequence, they
488 may be technique and even case-dependent^{27,28}. We believe it is important to use tests specif-
489 ically designed for dynamic treatments for characterizing and commissioning MLC models,
490 such as the recently proposed asynchronous sweeping gaps²⁰ and the trailing sweeping gaps
491 specific to the double-stacked MLC described in the present study. These tests facilitate
492 the configuration of MLC models in the TPS, standardizing the configuration process¹⁷ and
493 guiding future model developments²¹. MLC models that are able to reproduce the results
494 obtained with these dynamic tests should, in principle, provide a better accuracy in a wider
495 range of treatment techniques and plan characteristics. As an example, in RayStation 11P
496 configuring the system to reproduce the measured DLG for each MLC layer separately pro-
497 vided a good agreement not only for each independent layer, but also for the trailing effect
498 (see Figures 7 and 8).

499 The dose accuracy in clinical plans was not included in the current study, as it focused
500 on the characterization of the DLG and the trailing effect and their modeling in the TPSs.
501 However, several authors have already reported good dosimetric results in clinical Halcyon
502 plans with both Eclipse and RayStation^{12,29}. We believe that as MLC models evolve, helped
503 by detailed measurements including those in the current study, the dose calculation accuracy
504 in clinical plans will also improve, especially for cases with small dynamic leaf gaps and
505 trailing distances, which produced the largest discrepancies. Further improving the MLC

506 model and evaluating the benefits in clinical plans will be the subject of future work.

507 V. Conclusions

508 In the present study we described the previously unreported trailing effect in a stacked MLC
509 system, which is primarily due to the intricate interplay between the primary photon fluence
510 attenuation by the rounded leaf ends from different layers. This effect produces important
511 differences in the doses delivered by sweeping gaps with the HalcyonTM system depending
512 on the distance between the leaf tips from each layer (trailing distance). Additionally,
513 it also affects the measured DLG, which strongly depends on the arrangement used in its
514 determination. To maximize the DLG measurement accuracy it is important to use sweeping
515 gap plans that maintain the same MLC speed for different gap widths. This is not the case
516 with the DICOM RT Plan files currently supplied by the vendor.

517 The performance of a TPS in reproducing the trailing effect depended on the leaf tip
518 model implemented in each system. Eclipse has no explicit model of the leaf tip and could
519 not replicate this effect. RayStation implements a simple model of the leaf tip that could
520 partially replicate the trailing effect, especially with the modifications introduced in the
521 presented prototype.

522 The MLC dosimetric characteristics across five different Halcyon systems were quite
523 homogeneous, but differences around 0.2 mm were found in the measured DLG values.
524 The DLG for the proximal layer was always larger than for the distal one, on average by
525 0.16 ± 0.05 mm. A common preconfigured MLC model for the Halcyon system is feasible,
526 but these differences should ideally be taken into account by the TPS.

527 Double-stacked MLCs introduce new challenges such as the need for separate TPS
528 parameters for each MLC layer and the trailing effect, which should be carefully considered
529 when these systems are evaluated. The proposed trailing sweeping gap tests are useful for
530 characterizing and commissioning dual-layered MLCs.

531 Acknowledgments

532 Agnes Angerud is an employee of RaySearch Laboratories. The rest of the authors have no
533 conflicts to disclose.

534 Supporting information

535 Additional supporting information may be found online in the Supporting Information sec-
536 tion at the end of the article.

537 Data sharing

538 The data and DICOM files that support the findings of this study are available from the
539 corresponding author upon reasonable request.

540 References

542 ¹ L. Cozzi, A. Fogliata, S. Thompson, C. Franzese, D. Franceschini, F. de Rose, S. Tomatis,
543 and M. Scorsetti, Critical appraisal of the treatment planning performance of volumet-
544 ric modulated arc therapy by means of a dual layer stacked multileaf collimator for
545 head and neck, breast, and prostate, *Technology in cancer research & treatment* **17**,
546 1533033818803882 (2018).

547 ² R. De Roover, W. Crijns, K. Poels, S. Michiels, A. Nulens, B. Vanstraelen, S. Petillion,
548 M. De Brabandere, K. Haustermans, and T. Depuydt, Validation and IMRT/VMAT
549 delivery quality of a preconfigured fast-rotating O-ring linac system, *Medical Physics*
550 **46**, 328–339 (2019).

551 ³ T. Netherton et al., Experience in commissioning the halcyon linac, *Medical Physics*
552 **46**, 4304–4313 (2019).

553 ⁴ S. Gao, T. Netherton, M. A. Chetvertkov, Y. Li, L. E. Court, W. E. Simon, J. Shi,
554 and P. A. Balter, Acceptance and verification of the Halcyon-Eclipse linear accelerator-

- 555 treatment planning system without 3D water scanning system, *Journal of Applied Clin-*
556 *ical Medical Physics* **20**, 111–117 (2019).
- 557 ⁵ Y. Hu, M. Byrne, B. Archibald-Heeren, N. Collett, G. Liu, and T. Aland, Validation
558 of the preconfigured Varian Ethos Acuros XB Beam Model for treatment planning dose
559 calculations: A dosimetric study, *Journal of Applied Clinical Medical Physics* (2020).
- 560 ⁶ M. B. Sharpe, IAEA Technical Reports Series No. 430: Commissioning And Quality
561 Assurance Of Computerized Planning Systems For Radiation Treatment Of Cancer ,
562 *Medical Physics* (2006).
- 563 ⁷ I. J. Das, C.-W. Cheng, R. J. Watts, A. Ahnesjö, J. Gibbons, X. A. Li, J. Lowenstein,
564 R. K. Mitra, W. E. Simon, and T. C. Zhu, Accelerator beam data commissioning
565 equipment and procedures: report of the TG-106 of the Therapy Physics Committee of
566 the AAPM, *Medical Physics* **35**, 4186–4215 (2008).
- 567 ⁸ E. E. Klein et al., Task Group 142 report: Quality assurance of medical accelerators,
568 *Medical Physics* **36**, 4197–4212 (2009).
- 569 ⁹ G. A. Ezzell et al., IMRT commissioning: multiple institution planning and dosimetry
570 comparisons, a report from AAPM Task Group 119, *Medical Physics* **36**, 5359–5373
571 (2009).
- 572 ¹⁰ J. B. Smilowitz, I. J. Das, V. Feygelman, B. A. Fraass, S. F. Kry, I. R. Marshall,
573 D. N. Mihailidis, Z. Ouhib, T. Ritter, M. G. Snyder, and L. Fairobent, AAPM Medical
574 Physics Practice Guideline 5.a.: Commissioning and QA of Treatment Planning Dose
575 Calculations - Megavoltage Photon and Electron Beams, *Journal of Applied Clinical*
576 *Medical Physics* (2015).
- 577 ¹¹ K. Smith, P. Balter, J. Duhon, G. A. White Jr, D. L. Vassy Jr, R. A. Miller, C. F.
578 Serago, and L. A. Fairobent, AAPM Medical Physics Practice Guideline 8. a.: linear
579 accelerator performance tests, *Journal of Applied Clinical Medical Physics* **18**, 23–39
580 (2017).
- 581 ¹² A. Saini, C. Tichacek, W. Johansson, G. Redler, G. Zhang, E. G. Moros, M. Quyyum,
582 and V. Feygelman, Unlocking a closed system: dosimetric commissioning of a ring gantry

583

linear accelerator in a multi-vendor environment, *Journal of Applied Clinical Medical Physics* **x**, 1–14 (2021).

584

585

¹³ T. LoSasso, C.-S. Chui, and C. C. Ling, Physical and dosimetric aspects of a multileaf collimation system used in the dynamic mode for implementing intensity modulated radiotherapy, *Medical Physics* **25**, 1919–1927 (1998).

586

587

588

¹⁴ M. M. Kim, D. Bollinger, C. Kennedy, W. Zou, R. Scheuermann, B.-K. K. Teo, J. M. Metz, L. Dong, and T. Li, Dosimetric Characterization of the Dual Layer MLC System for an O-Ring Linear Accelerator, *Technology in cancer research & treatment* **18**, 1533033819883641 (2019).

589

590

591

592

¹⁵ T. Y. Lim, I. Dragojević, D. Hoffman, E. Flores-Martinez, and G.-Y. Kim, Characterization of the Halcyon™ multileaf collimator system, *Journal of Applied Clinical Medical Physics* **20**, 106–114 (2019).

593

594

595

¹⁶ M. R. Arnfield, J. V. Siebers, J. O. Kim, Q. Wu, P. J. Keall, and R. Mohan, A method for determining multileaf collimator transmission and scatter for dynamic intensity modulated radiotherapy, *Medical Physics* **27**, 2231–2241 (2000).

596

597

598

¹⁷ J. Saez, V. Hernandez, J. Goossens, G. De Kerf, and D. Verellen, A novel procedure for determining the optimal MLC configuration parameters in treatment planning systems based on measurements with a Farmer chamber, *Physics in Medicine & Biology* (2020).

599

600

601

¹⁸ X. Mei, I. Nygren, and J. E. Villarreal-Barajas, On the use of the MLC dosimetric leaf gap as a quality control tool for accurate dynamic IMRT delivery, *Medical Physics* **38**, 2246–2255 (2011).

602

603

604

¹⁹ J. F. Dempsey, H. E. Romeijn, J. G. Li, D. A. Low, and J. R. Palta, A Fourier analysis of the dose grid resolution required for accurate IMRT fluence map optimization, *Medical Physics* **32**, 380–388 (2005).

605

606

607

²⁰ V. Hernandez, J. A. Vera-Sánchez, L. Vieilleveigne, and J. Saez, Commissioning of the tongue-and-groove modelling in treatment planning systems: from static fields to VMAT treatments, *Physics in Medicine & Biology* **62**, 6688 (2017).

608

609

- 610 21 V. Hernandez, J. A. Vera-Sánchez, L. Vieillevigne, C. Khamphan, and J. Saez, A new
611 method for modelling the tongue-and-groove in treatment planning systems, *Physics in*
612 *Medicine & Biology* **63**, 245005 (2018).
- 613 22 Varian Medical Systems, Eclipse Photon and Electron Reference Guide, (2019).
- 614 23 RaySearch Laboratories, RayStation 10A Reference Manual, (2020).
- 615 24 P. Zygmanski, F. Rosca, D. Kadam, F. Lorenz, A. Nalichowski, L. Court, and L. Chin,
616 Determination of depth and field size dependence of multileaf collimator transmission
617 in intensity-modulated radiation therapy beams, *Journal of Applied Clinical Medical*
618 *Physics* **8**, 76–95 (2007).
- 619 25 K. N. Kielar, E. Mok, A. Hsu, L. Wang, and G. Luxton, Verification of dosimetric
620 accuracy on the TrueBeam STx: rounded leaf effect of the high definition MLC, *Medical*
621 *Physics* **39**, 6360–6371 (2012).
- 622 26 L. Vieillevigne, C. Khamphan, J. Saez, and V. Hernandez, On the need for tuning the
623 dosimetric leaf gap for stereotactic treatment plans in the Eclipse treatment planning
624 system, *Journal of Applied Clinical Medical Physics* **20**, 68–77 (2019).
- 625 27 S. Szpala, F. Cao, and K. Kohli, On using the dosimetric leaf gap to model the rounded
626 leaf ends in VMAT/RapidArc plans, *Journal of Applied Clinical Medical Physics* **15**,
627 67–84 (2014).
- 628 28 J. Kim, J. S. Han, A. T. Hsia, S. Li, Z. Xu, and S. Ryu, Relationship between dosi-
629 metric leaf gap and dose calculation errors for high definition multi-leaf collimators in
630 radiotherapy, *Physics and Imaging in Radiation Oncology* **5**, 31–36 (2018).
- 631 29 E. Laugeman et al., Comprehensive validation of halcyon 2.0 plans and the implementa-
632 tion of patient specific QA with multiple detector platforms, *Journal of Applied Clinical*
633 *Medical Physics* **21**, 39–48 (2020).

Institution	TPS	Algorithm	Phantom
Centre Oscar Lambret, Lille, France (A)	RayStation 9A	CC	Water (MPI, PTW)
Institut Sainte Catherine, Avignon, France (B)	Eclipse 15.6	AAA	Water (myQA HALO™, IBA)
IUCT Oncopole, Toulouse, France (C)	Eclipse 15.6	AAA	Water (BeamScan™, PTW)
Moffitt Cancer Center, Florida, USA (D)	RayStation 9B	MC	Plastic (Plastic Water®, CIRS)
Radiotherapy Center of Mâcon, France (E)	Eclipse 15.6	AAA	Water (1D SCANNER™, Sun Nuclear)
	RayStation 10A	CC	

Table 1: Institutions and equipment used in the study. The dose calculation algorithms were: Anisotropic Analytical Algorithm (AAA), Collapsed Cone (CC) and Monte Carlo (MC).

Institution	Proximal layer (upper)		Distal layer (lower)		Both layers	
	DLG (mm)	T	DLG (mm)	T	DLG (mm)	T
A	0.47	0.32%	0.32	0.34%	-0.44	0.006%
B	0.46	0.33%	0.28	0.34%	-0.48	0.005%
C	0.36	0.32%	0.12	0.34%	-0.62	0.005%
D	0.42	0.32%	0.28	0.33%	-0.48	0.005%
E	0.48	0.32%	0.38	0.33%	-0.42	0.005%
Average	0.44	0.322%	0.28	0.336%	-0.49	0.005%
Standard deviation	0.05	0.002%	0.10	0.003%	0.08	0.0003%

Table 2: Dosimetric leaf gap (DLG) and transmission (T) obtained at each institution for each layer and both layers combined.

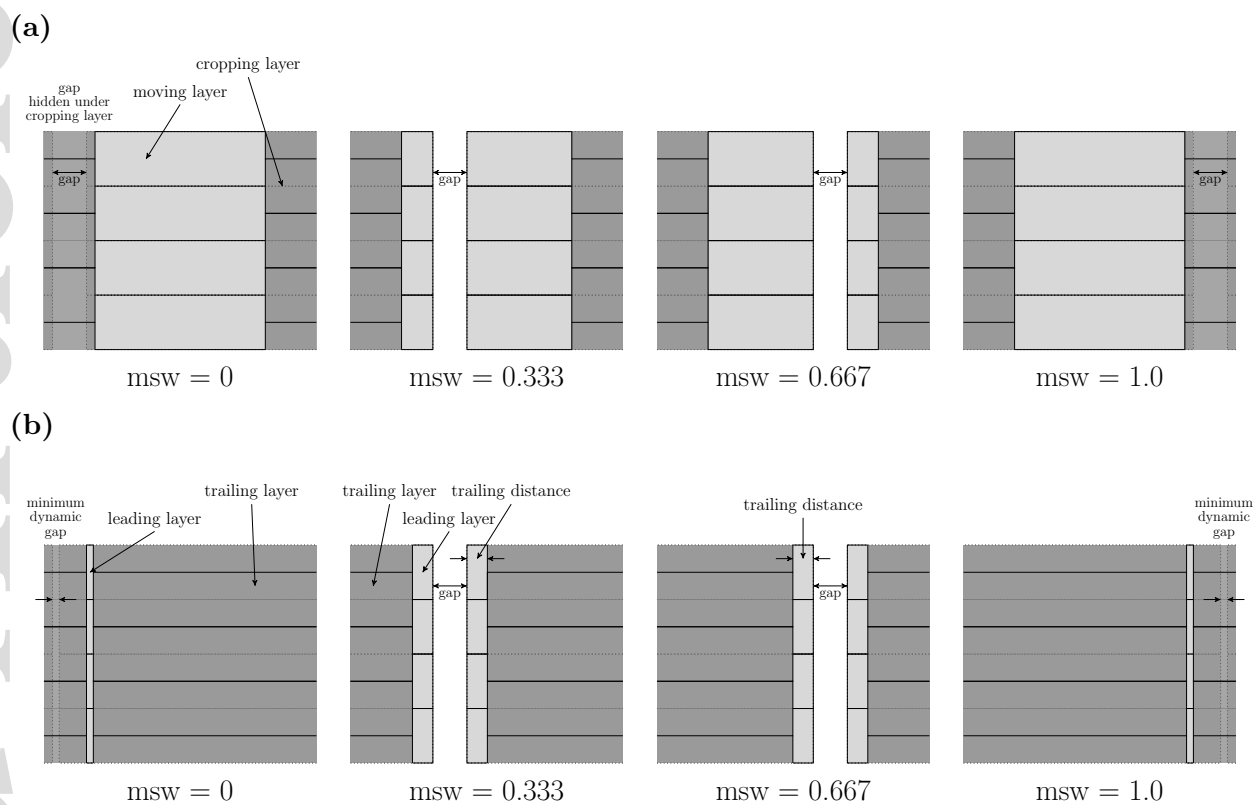


Figure 1: Sketch illustrating (a) the sweeping gap test and (b) the trailing sweeping gap test in the beam's eye view. The leaf positions are shown for different meterset weights (msw). Two versions of the tests were designed with the proximal and distal layers interchanging the leading and trailing roles.

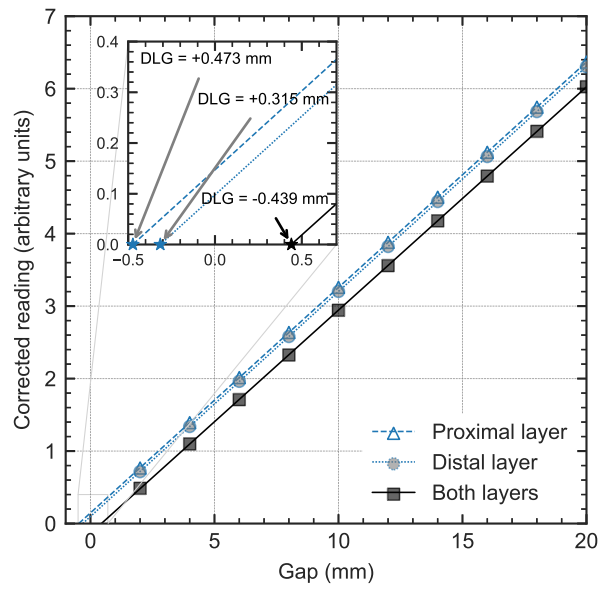


Figure 2: Results of the sweeping gap tests for the proximal and distal layers and for both layers combined (center A). The corrected readings (after subtracting MLC transmission) are plotted as a function of the gap size. The negative of the x-axis intercept of the linear fit defines the dosimetric leaf gap (DLG).

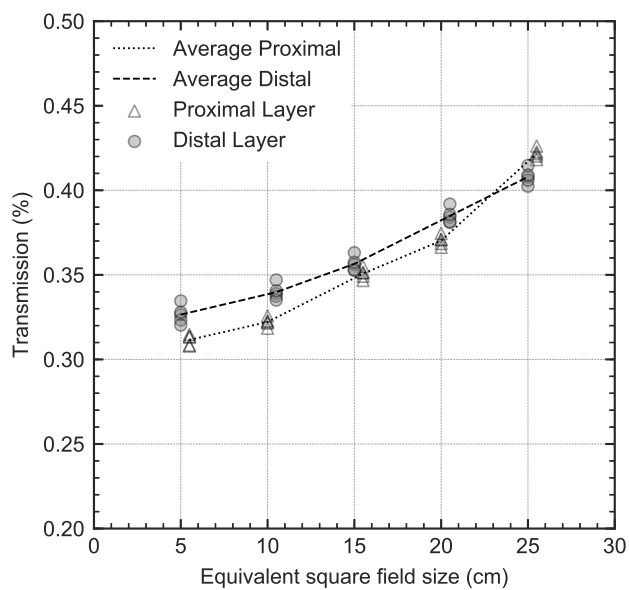


Figure 3: MLC transmission as a function of the field size. Symbols represent the values measured at each institution and dashed lines indicate the average values.

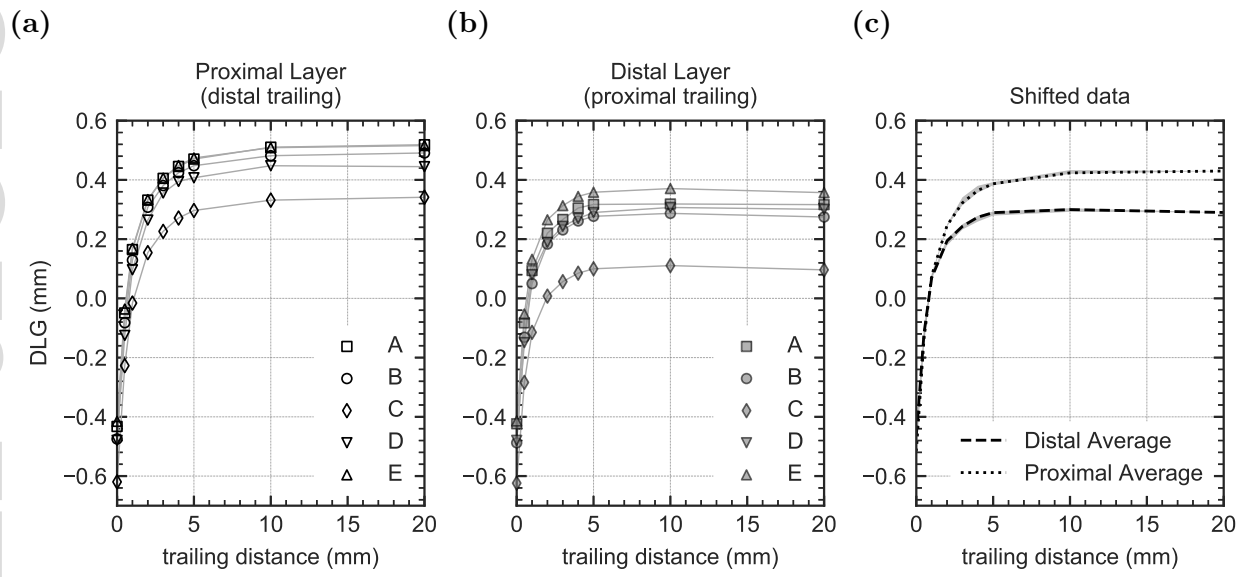


Figure 4: Dosimetric leaf gap (DLG) values obtained at the five institutions as a function of the trailing distance t for the (a) proximal and (b) distal layers. In (c) the DLG curves from each institution were shifted vertically so that the DLG for $t = 20$ mm matches the average DLG given in Table 2. The lines in (c) represent the average curves and the shaded areas indicate the range of variability between different institutions.

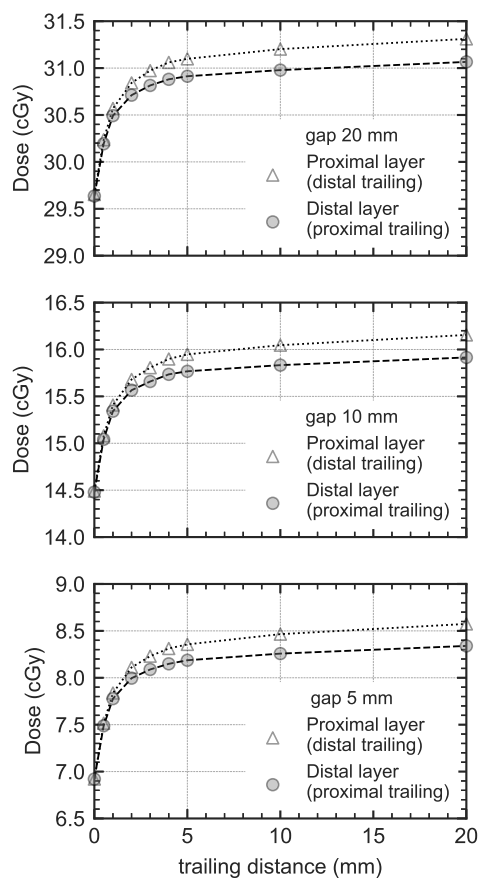


Figure 5: Measured sweeping gap doses as a function of the trailing distance for different gap sizes. A common dose scale was used in all plots to illustrate that dose variations were independent of the gap size. The doses shown correspond to 100 MU.

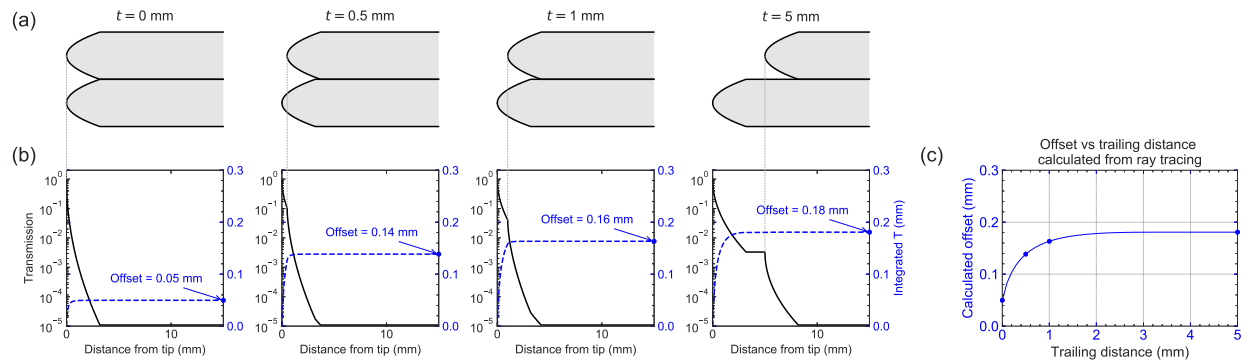


Figure 6: Results obtained with ray tracing. In (a) a sketch of the leaves from each layer for different trailing distances is illustrated. The computed transmission through the leaves and the corresponding integral transmission (dashed lines) are shown in (b). In (c) the leaf offset computed with ray tracing is plotted as a function of the trailing distance.

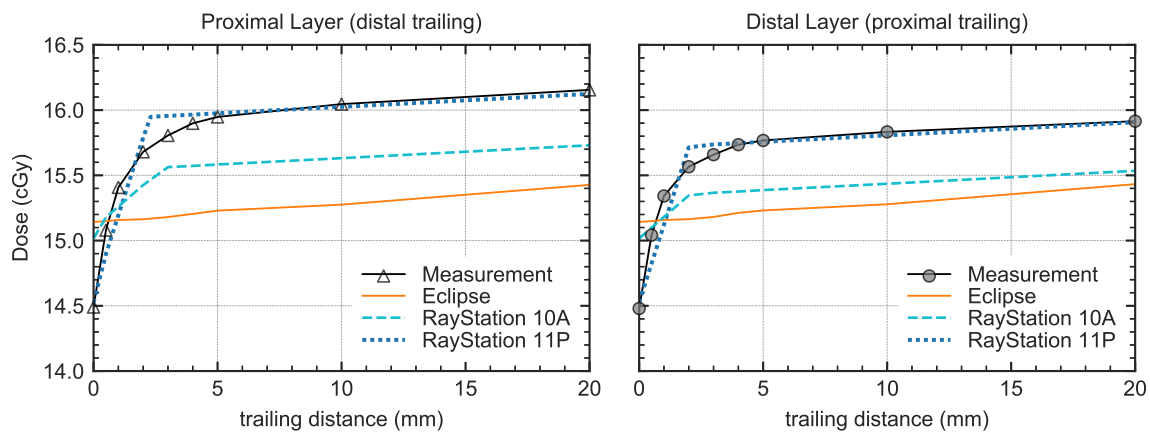


Figure 7: Measured and calculated doses for a 10 mm sweeping gap as a function of the trailing distance. The doses shown correspond to 100 MU.

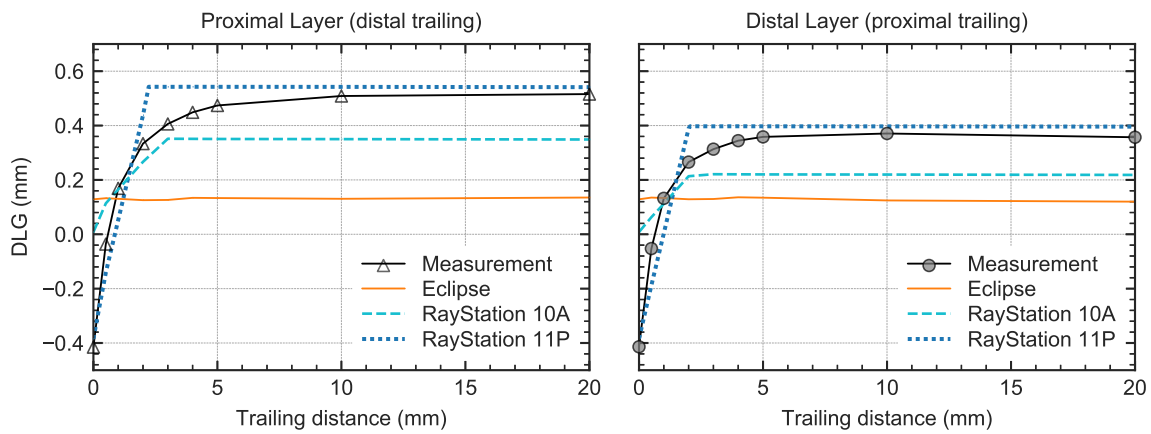


Figure 8: Dosimetric leaf gap (DLG) values obtained from measurements and calculations from the Eclipse and RayStation treatment planning systems for the proximal and distal layers, as a function of the trailing distance.